

Geometric Properties of Ising model on an Interacting Self-Avoiding Walks

Ilya Pchelintsev, Kamilla Faizullina, Evgeni Burovski

HSE University, 101000 Moscow, Russia

Abstract. This is an abstract and that's really abstract.

1. Introduction

The model of self-avoiding walks is one of extensively studied examples of linear polymers. Moreover, it is the simplest model to study critical behaviour while other models polymer chains have different states in the thermal equilibrium in various solvent conditions. By adding interaction between nearest neighbors of monomers of the walk, we are allowed to study phase transition fixed between solvent conditions, so the given polymer in the thermal equilibrium become extended in good-solvent conditions and collapsed in poor-solvent one. This tricritical nature was described in Ref.[1].

The impact of close-range interaction was studied precisely in models of magnetic polymers, where interaction between monomers became more complex after each monomer carried a spin and strength of nearest neighbors coupling became variable. This is so called Ising Model on a SAW conformation. In Ref.[2], the model was complicated by adding external magnetic field and all conclusions about magnetic properties were by comparing with mean-field model. However, there are some geometric properties which impact of magnetic properties is not clear while studying of require more brute methods.

In previous studies, it was established that Ising model on the self-avoiding walk conformations (SAWs) has a continuous type of phase transition [3]. In this work, we continue study geometric properties of this model and compare them with "parent" models and its modifications, such as Ising model on the rectangular lattice, considered in Ref.[4], and two-dimensional interacting self-avoiding walks exactly in their respective critical regions. We suggest that models with similar geometric properties will also have same magnetic properties, what we suggest to observe in comparing values of Binder cumulants in the θ -transition of models with the equal values of asphericities.

2. Models and Methods

In the paper we consider several models: the first one is Ising model on interacting self-avoiding walk from Ref. [3], on three different lattices: 2D-square lattice, 3D-square lattice and 2D-triangular lattice. The main difference between square and triangular lattice in defining two additional diagonal monomers on lattice as nearest too. Considering the case of lack of outer magnetic field in this work, the Hamiltonian of the model of fixed conformation u with length N and strength of nearest-neighbors interaction J reads:

$$H_{u,N,\{\sigma\}} = - \sum_{\langle i,j \rangle} J \sigma_i \sigma_j, \quad i, j \in u, \quad |u| = N \quad (1)$$

The summation runs through spins involved in conformation and only with the nearest neighbors.

The equilibrium partition function corresponding to Eq. (1) reads

$$Z = \sum_{u \in \mathcal{U}_N} \sum_{\{\sigma\}} e^{-\beta H_{u,N,\{\sigma\}}}, \quad (2)$$

where β is the inverse temperature.

The second model considered in this paper is the Ising model on the rectangular lattice from the Ref.[4]. Simulated lattices has $L \times rL$ spins and the Hamiltonian is calculated through interaction between all spins and their nearest neighbors respectively:

$$H_{L,r,\{\sigma\}} = - \sum_{\langle i,j \rangle} J \sigma_i \sigma_j \quad (3)$$

Here the i -th spin of the lattice has a pair of coordinates from $[1..L] \times [1..rL]$. For comparing magnetic properties of models with similar geometric ones we also define shape factors, such as gyration tensor of system with N points w_i [5]:

$$Q_{N,\alpha\beta} = \frac{1}{N} \sum_{i=1}^N (w_{i,\alpha} - w_{c,\alpha})(w_{i,\beta} - w_{c,\beta}) \quad (4)$$

where N is length of the system (number of monomers in conformations of Ising-ISAW models or number of spins in the lattice in rectangular Ising), and $w_{i,\alpha}, w_{i,\beta}$ are the coordinates of i -th point of conformation. $w_{c,\alpha}, w_{c,\beta}$ are coordinates of the center of system (so, $Q_{N,xx}$ and $Q_{N,yy}$ can be defined as mean squares of coordinates of the points of the model in the cartesian coordinate system with the center in the center of model). Eugen values $q1, q2$ of given tensor can be interpreted as $Q_{N,xx}$ and $Q_{N,yy}$ in the coordinate system of eugen vectors, or more important - as square of semi-axes of ellipse of inertia of given system. The proportion of them for systems with length N will be [5]:

$$r = \sqrt{\frac{\langle q1 \rangle_N}{\langle q2 \rangle_N}} \quad (5)$$

Eugen values $q1, q2$ are also used in enumerating another important shape factor - mean asphericity [5]:

$$\mathcal{A} = \left\langle \frac{(q1 - q2)^2}{(q1 + q2)^2} \right\rangle_N \quad (6)$$

The compared magnetic property of our models is the fourth order cumulant of the magnetization of the Binder cumulant, defined as [6]:

$$U_4 = 1 - \frac{\langle m^4 \rangle}{3 \langle m^2 \rangle^2} \quad (7)$$

Where $\langle m^4 \rangle$ and $\langle m^2 \rangle$ are mean fourth and second order of mean magnetization per spin respectively.

We also need to define mean proportion of monomers with fixed number i of nearest neighbors $\langle n_i \rangle$, which is counted directly for every monomer in every simulated conformation of walk.

We are interested in comparing models in their respective critical regions. For each structure, critical temperatures of Ising models are known as:

Structure	lattice	J_c
ISAW conformation	Square	$0.8340(5)[3]$
ISAW conformation	Cubic	$0.5263 \pm 0.055[7]$
Regular lattice	Rectangular	$\ln(1 + \sqrt{2})/2[8]$

Table 1: Known values of critical temperature of different modifications of Ising-ISAW model and normal Ising on the rectangular lattice

lattice	T_c
Square	$0.6673(5) [5]$
Cubic	$0.2779 \pm 0.0041[9]$
Triangular	$0.405 \pm 0.07[10]$

Table 2: Known values of critical temperature of different modifications of ISAW model

3. Results

3.1. Mean Asphericity and Critical Cumulant

We attempted to learn how magnetic properties of Ising-like models depend on their geometrical ones and to define their comparability in critical region, where dependence of observable values of models with the length of conformation N is the weakest. The idea is to compare critical cumulants $U_4(7)$ of both models of Ising having equal asphericities. Both models are considered to have open boundary conditions (OBC). As we know, in the Ising model on rectangular lattice shape factors like aspect ratio r are the parameters, not observable values. Therefore, we can find value of the aspect ratio of lattice for any asphericity \mathcal{A} (6) (see fig. 2). For rectangular lattice, the leading correction term to the asphericity behave like $A^*(r) - A(r, L) \propto 1/L^2$. Moreover, we know that value of Binder cumulant in Rectangular Ising in critical region depends on aspect ratio r [4].

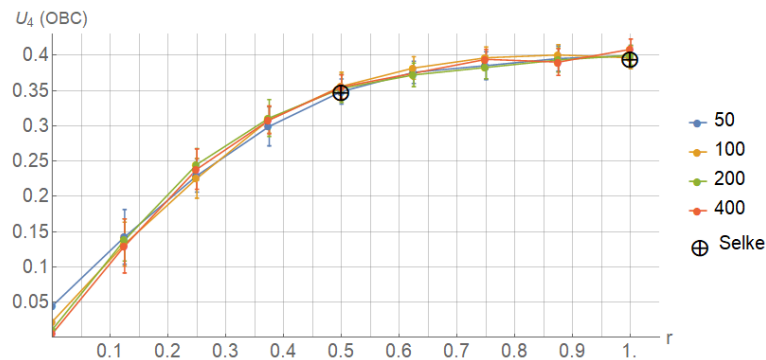


Figure 1: Critical cumulant $U_4(7)$ of Ising model on a rectangular lattice with open boundary conditions as function of aspect ratio r with side length $L = 50$ (blue), 100 (yellow), 200 (green) and 400 (red). Black markers define values from [4]

Performing Monte-Carlo simulations with steps of Wolff algorithm [11] on Ising model on a rectangular lattice with open boundary conditions in θ -point ($J_c = \ln(1 + \sqrt{2})/2 = 0.44068\dots$), we collected statistics for Binder cumulant U_4 with respect to aspect ratio r (see table 1). Our results matched with known values from Ref. [4].

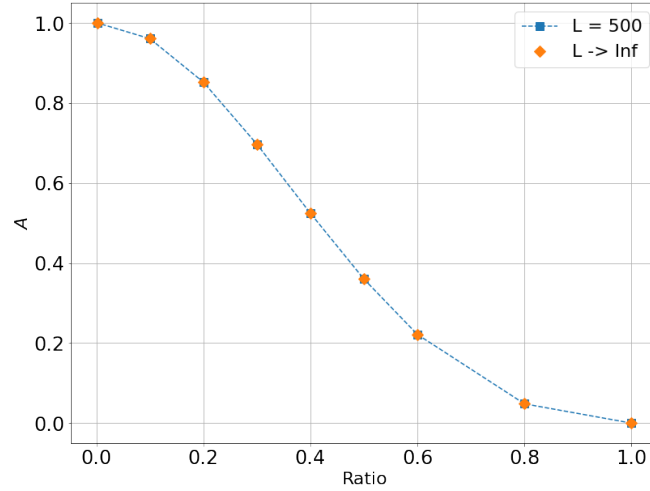


Figure 2: Asphericity as function of aspect ratio r of the rectangular lattice with side length = 500 and approximate values for rectangular lattice with infinitely long side

We also simulated Ising-ISAW and ISAW model on 2D-square lattice for lengths $N = 1000-4900$. We used method described in [3]. Our simulations were performed for $0 < J < 1$, focusing on areas near respective critical regions.

Figure 3 shows results of our simulations for asphericity (6) as function of J . For ISAW model $J_c = 0.6673(5)$, and our result are matching to known values from Ref. [5], where critical region was also enumerated. For Ising-ISAW model we used our value from previous work: $J_c = 0.8340(5)$ [3] and for border values we used values from Ref.[7] ($J_c = 0.8340 \pm 0.0021$). Both values were marked as black vertical lines with blue zone around, which will define all statistical errors of critical regions. Horizontal line define value of critical asphericity of ISAW model, which is known from Ref. [5], which our results for ISAW model matches with.

We took mean values of asphericity of Ising-ISAW model in the borders of critical region and in the point of the best crossing of plots where we observe phase transition according to our numerical results. All these points are marked as black in zoomed figures 4. Our following steps was to pick up values of aspect ratio, to perform simulations of the Rectangular Ising with the same ratio and, consequently, asphericity and to find critical cumulant of the model with the same shape factors. As it seen from fig. 2, it is enough to use lattice with length $N = 500$ for picking up the aspect ratio. For simulations we used cluster update based on Wolff algorithm [11] on a rectangular lattice with the same length.

As a result, comparison with critical cumulant of Ising-ISAW model, which value was found during simulations in Ref.[3] ($U_4 = 0.308(8)$) showed significant mismatch of values, which means that we had not took into account some other geometrical properties - for example, which will be considered in the next part - proportions of monomers with different quantities of nearest neighbors. It is obvious that in Ising model on the rectangular lattice most of monomers located

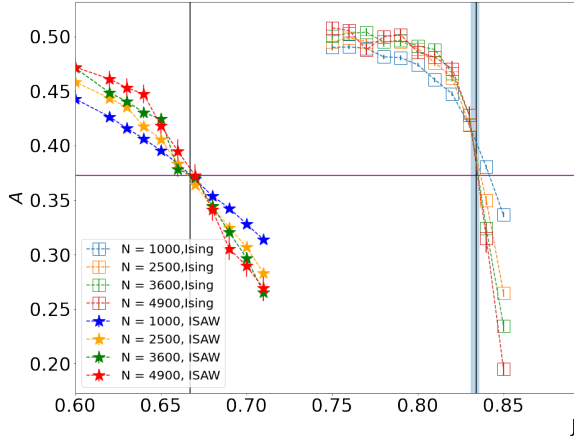


Figure 3: Asphericity of Ising-ISAW (empty squares) and ISAW-only models (stars) as function of $J = 1/T$, varying lengths of conformations $N = 1000$ (blue), 2500 (yellow), 3600 (green) and 4900 (red)

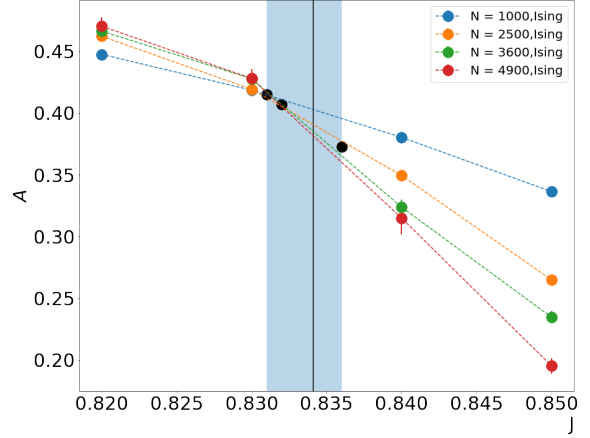


Figure 4: Asphericity of Ising-ISAW model as function of zoomed in the critical region (blue zone, according to Ref. [7] and black vertical line, according to Ref. [3]), varying lengths of conformations $N = 1000$ (blue), 2500 (yellow), 3600 (green) and 4900 (red)

Ising-ISAW			
J	\mathcal{A}	r	U_4 <i>Rectangular</i>
0.831	0.415	0.465	0.338 ± 0.006
0.832	0.4072	0.47	0.343 ± 0.006
0.836	0.373	0.492	0.349 ± 0.006

Table 3: Values of critical cumulant for Ising model on rectangular lattice with mean asphericity related to Ising-ISAW model in its critical region

inside the lattice and have 4 nearest neighbors, while monomers spread around the perimeter of the lattice have at least 2 (corners) and 3 nearest neighbors. Proportions in Ising-ISAW conformations are completely different (see fig. 7).

3.2. Bulk-to-surface ratios

Typical ISAW conformations (see Fig. ??) in the θ -critical region can be thought of having a blob-and-link structure. Above the θ temperature, blobs have a finite size and are separated; at the transition, all blobs merge. In the collapsed phase, the free energy energy acquires a surface term [12]. While the notion of a surface is only well-defined in the collapsed phase, surface-like corrections are large around the θ point for a 2D ISAW model [13]. In order to quantify surface-like effects across the transition, we follow Ref. [3] and consider local connectivity of internal monomers in a conformation. Specifically, for each monomer in a conformation we count the number of monomers on its nearest neighbor sites and classify each monomer as “1D-like” (two neighbors), “2D-like” (four neighbors) or “surface-like” (three neighbors), see Fig. 5 for an illustration.

Denoting by n_α the fraction of monomers with α neighbors, for a length- N conformation on

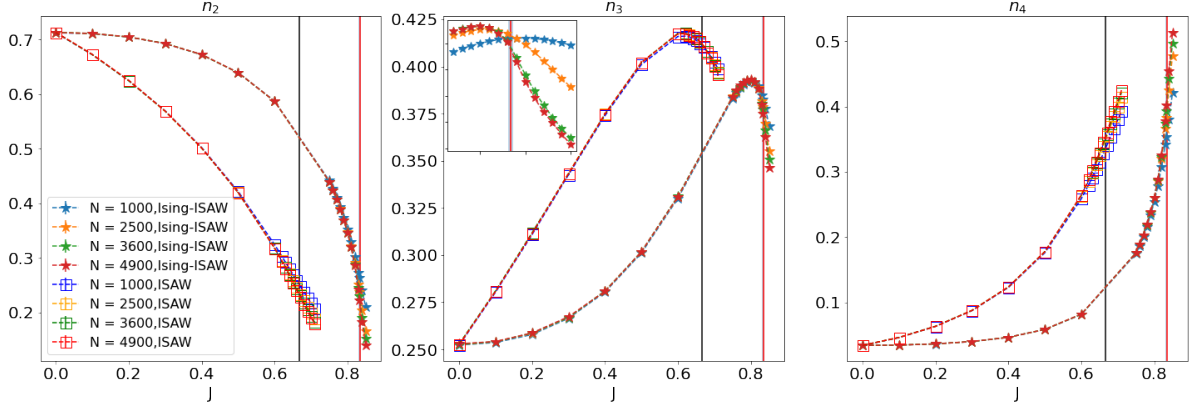


Figure 7: Fractions of monomers of Ising-ISAW model (squares) and ISAW model (stars) on a square lattice with 2-4 nearest neighbors as function of J with length of conformations $N = 1000$ (blue), 2500 (yellow), 3600 (green), 4900 (red). Black vertical line define point of θ -transition for ISAW model [5], red line - for Ising-ISAW model [3, 7]. Reproduced from Ref.[3]

Fig. 7 shows results of MC simulations for n_α as functions of the coupling constant J across the collapse transition for both ISAW model and Ising-ISAW model (??). We see that for the lengths $N > 1000$, finite-size corrections are barely visible. For the ISAW model, the fraction of the “2D-like” monomers, n_4 , is essentially zero for small J and quickly increases on approach to the θ -point. For the Ising-ISAW model, the behavior is qualitatively similar, if somewhat more smooth for $J < J_\theta$. The “1D-like” fraction, n_2 is also a smooth monotonic function across the whole range of J .

On the contrary, the “surface-like” fraction, n_3 ,—for both models—develops a peak in the vicinity of the respective collapse transitions. The available MC data suggest that the peak becomes more narrow as N increases, and that the position of the peak is shifted away from the θ -point.

3.2.2. 3D cubic lattice ($z = 6$) On a 3D cubic lattice with the coordination number $z = 6$, the classification of a local neighborhoods is more complicated than that on a 2D square lattice. “1D-like” monomers still have two neighbors, deep bulk corresponds to six neighbors. Considering a cube-shaped globule, three neighbors define “corners”, and faces of a cube have five neighbors. Since typical conformations are not perfect cubes, it is reasonable to expect that n_6 corresponds to the “bulk-like” monomers and n_3 , n_4 and (to some extent) n_5 correspond to “surface-like” monomers.

Fig. 8 shows our MC results for the 3D cubic lattice in the left column. Here we simulate conformations of up to $N = 600$ for both models, Ising-ISAW ?? and ISAW ??.

For the Ising-ISAW model, Fig. 8 shows that the “1D-like” and “bulk-like” fractions, n_1 and n_6 , respectively, are monotonic and develop a jump at the critical coupling at increasing N , which is consistent with the first-order character of the transition [2, 7].

The “surface-like” fractions n_3 and n_4 clearly develop a peak in the critical region, which becomes progressively more narrow and better defined at increasing N , Finite-size corrections are strong for the available values of N .

Our MC data for n_5 can be interpreted as finite- N corrections to either a jump or a peak. Simulations for larger lengths N are needed to conclusively resolve the behavior of n_5 in the critical region.

For the ISAW model the behavior is qualitatively similar: the “bulk-like” fraction, n_6 , is

essentially zero all the way up to the theta-transition $J_\theta = \dots$ and is monotonically increasing for $J > J_\theta$, the “1D-like” fraction n_2 decreases monotonically with J —for the available lengths N , the behavior is almost featureless. The “surface-like” fractions n_3 and n_4 develop a peak which shifts towards J_θ as N increases, and n_5 is very slowly developing what is probably a peak. The overall dependence of n_α on J for the available lengths $N \leq 600$ is much slower for the ISAW model than for the Ising-ISAW model, which is consistent with a continuous collapse transition with tricritical exponents [?].

Comparing the behavior of the ISAW and Ising-ISAW models on the 3D cubic lattice, we conclude that the dependence of the “surface-like” fraction is sensitive to the nature of the collapse transition: for the ISAW model, where the transition is continuous, the finite-size corrections are much stronger than those for the Ising-ISAW model, where the transition is first-order. **XXX: into the conclusion**

TODO: 0.25, hypercubic

3.2.3. 2D triangular lattice ($z = 6$) In this section, we consider the ISAW and Ising-ISAW models on the 2D triangular lattice, which has a coordination number $z = 6$. Despite having the same coordination number as a 3D cubic lattice, the triangular lattice structure is rather different for the SAW-like conformations because a one-dimensional line forms and impenetrable boundary on a triangular lattice but not on a cubic lattice. Monomers with one and six neighbors still can be interpreted as “1D-like” and “bulk-like”, respectively, but the straight boundary corresponds to four neighbors. This way, the interpretation of the fraction n_3 is not entirely clear-cut: it is neither “1D-like”, nor does it correspond to a right boundary. We can thus expect that the “surface-like” behavior is displayed by the fractions n_4 and n_5 .

Fig. 8 shows results of MC simulations in the right-hand column. For the ISAW model (open symbols) the fractions n_2 and n_3 are monotonically decreasing functions of J . The “surface-like” fractions, n_4 and n_5 develop broad peaks which get progressively sharper with increasing N . The peak locations are not far from the estimate of the collapse transition $J_t = 0.405 \pm 0.07$ of Ref. [10]. The bulk fraction n_6 is a featureless monotonically increasing function of J for the available lengths $N \leq 600$.

For the Ising-ISAW model the behavior is qualitatively similar, with the location of the peaks of n_4 and n_5 suggesting that the collapse transition occurs around $J_t \approx 0.6$. We are not aware of an independent estimate of the location of the collapse transition for the Ising-ISAW model on a triangular lattice.

Comparing the Ising-ISAW and ISAW models, we see that in the latter model, the finite-size dependence is smoother than in the former, suggesting that the crossover exponent, which governs the size of the critical region, is larger for the ISAW model.

Finally, we consider the $J = 0$ limit. **1. No 1/4 — specific for hypercubic lattices? 2. Note that $n=2$ and $n=3$ are both equal 0.36, are they?**

In this section we studied proportions of monomers with fixed numbers of nearest neighbors for Ising-ISAW and ISAW models on 3D-square and 2D-triangular lattices. Monomers of all four modified models can have from 2 to 6 close-range energy connections and some types of monomers, according to number of connections they have, can be interpreted similarly: for example, it is obvious that parts of conformations with monomers with only two nearest neighbors represent 1D-conformations or chains whatever lattice was used in observed model. And the opposite - regions where monomers have maximum number of close-range connections represent densely packed areas deep inside the globule. Talking about cubic lattice, other types of monomers can be also interpreted: monomers with only three neighbors define “corners” on conformation, while only monomers on a cube edge (or it also can be on a isolated plane from other part of globule) can have four neighbors. Presence on five neighbors belongs to the

monomers on a surface of conformation. Unfortunately, we cannot make similar interpretations for conformations on a triangular lattices.

To begin with, we performed simulations of ISAW model on square lattice on lengths from 5 to 3600 at $J = 0$ with collecting statistics for fraction of monomers with 2 to 4 neighbors. To understand we mechanics of calculating neighbors of monomers, we also manually enumerated fractions of monomers with these number of neighbors for short conformations (5 to 11). Our results matched.

3.2.4. Ising model on a SAW-conformation Using method of MC simulations from Ref. [3], we enumerated proportions of monomer with 2-6 nearest neighbors in Ising-ISAW model on a three-dimensional square (or cubic) lattice.

As it is seen from left part of Figure 8, increasing the strength of nearest-neighbors interaction J leads to conformation becoming more dense as proportions of monomers with higher numbers of close-range connections significantly increases after θ -transition located in a blue zone (for Ising-ISAW model on a cubic lattice $T_c = 0.5263 \pm 0.055$ [7]) (see Table 1).

We also repeated MC simulations for two-dimensional triangular lattice. Unlike the 3D-square lattice, the 5-th and 6-th possible neighbors located on the same plane as the first four, so conformations are expected to be more dense on this lattice.

TODO: include Critical region of the model on a triangular lattice was not enumerated yet. But as it was suggested, density of conformations becomes higher as nearest-neighbors interaction J strengthen. Moreover, proportion of monomers with six neighbors on a triangular lattice is far higher than on a cubic one. It is also significant that "triangular" conformations with no inner interaction have almost twice shorter one-dimensional chains than conformations on a cubic lattice in the same conditions.

3.2.5. ISAW model To understand how the presence of magnetic properties affects on density of models, we also performed Monte-Carlo simulations on a parental model of self-avoiding walks on the same lattices. Results was similar to Ising-ISAW model, as suggested from "parent" model. For cubic lattice $T_c = 0.2779 \pm 0.0041$ [9]. For the triangular lattice, $J_c = 0.405 \pm 0.07$ [10]. Figure 8 shows that geometric aspects of phase transition in ISAW model manifest earlier than in Ising-ISAW ones.

4. Discussion

5. Acknowledgments

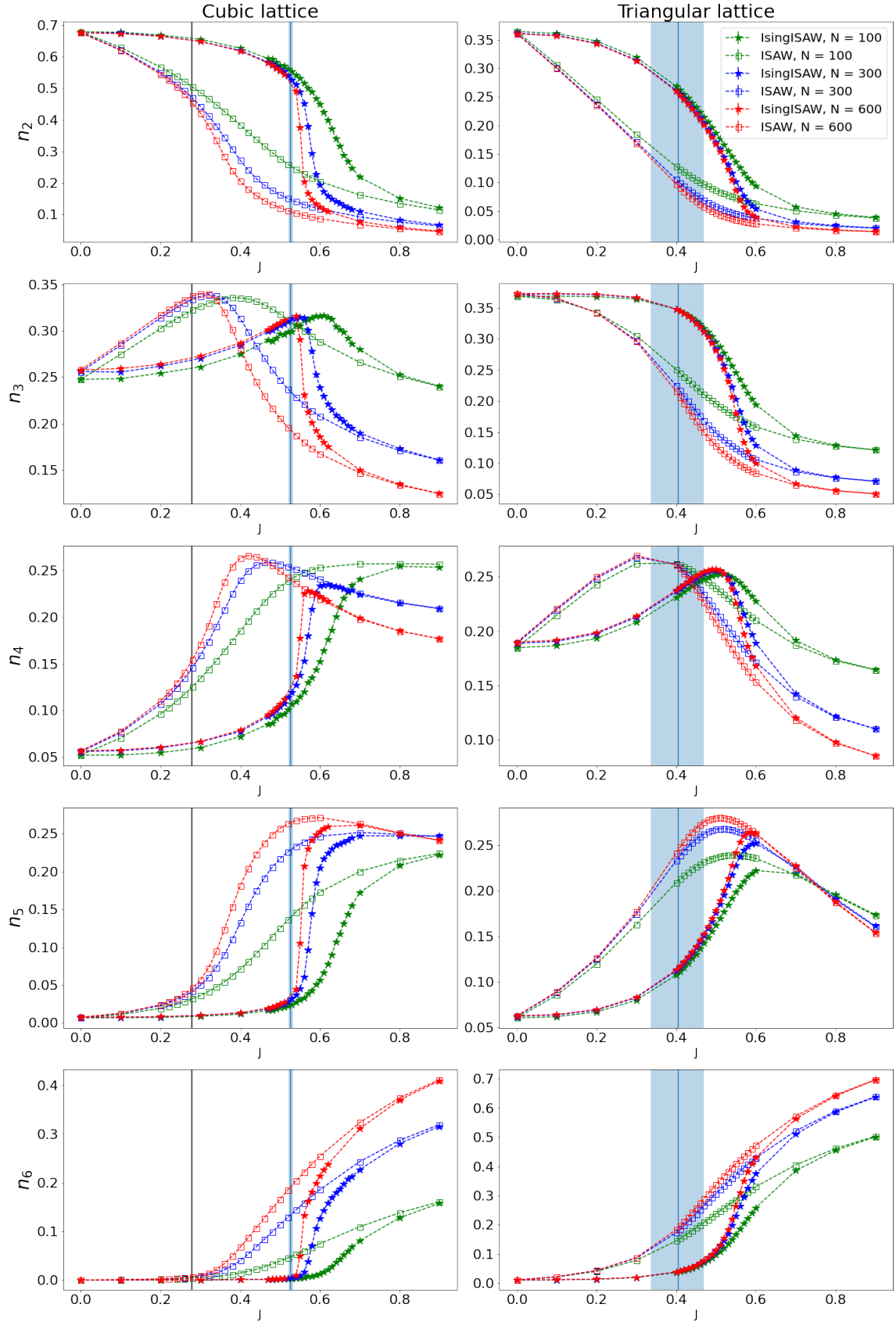


Figure 8: Fractions of monomers of Ising-ISAW model (stars) and ISAW model (open squares) on a cubic lattice (left column) and 2D-triangular lattice (right column) with 2-6 nearest neighbors as function of J with length of conformations $N = 100$ (green), 300 (blue) and 600 (red). Vertical lines define points of θ -transition (For cubic lattice: black line for ISAW model [9] and blue line for Ising-ISAW model [7]; for triangular lattice: blue line for ISAW model [10])

- [1] de Gennes P G 1979 *Scaling concepts in polymer physics* (Cornell University Press)
- [2] Garel T, Orland H and Orlandini E 1999 *Eur. Phys. J. B* **12** 261–268
- [3] Faizullina K, Pchelintsev I and Burovski E 2021 (*Preprint* 2107.11830)
- [4] Selke W 2006 *Eur. Phys. J. B* **51** 223–228 ISSN 14346028 (*Preprint* 0603411)
- [5] Caracciolo S, Gherardi M, Papinutto M and Pelissetto A 2011 *J. Phys. A: Math. Theor.* **44** 1–24 ISSN 17518113 (*Preprint* 1012.1177)
- [6] Binder K 1981 *Z. Phys. B* **43** 119
- [7] Foster D and Majumdar D 2021 *Phys. Rev. E* **104**(2) 024122 URL <https://link.aps.org/doi/10.1103/PhysRevE.104.024122>
- [8] Onsager L 1944 *Phys. Rev.* **65**(3-4) 117–149 URL <https://link.aps.org/doi/10.1103/PhysRev.65.117>
- [9] Tesi M C, van Rensburg E J J, Orlandini E and Whittington S G 1996 **29** 2451–2463 URL <https://doi.org/10.1088/0305-4470/29/10/023>
- [10] Privman V 1986 *J. Phys. A: Math. Gen* **19** 3287–3297 URL <https://doi.org/10.1088/0305-4470/19/16/027>
- [11] Newman M E J and Barkema G T 1999 *Monte Carlo methods in statistical physics* (Oxford: Clarendon Press)
- [12] Owczarek A L, Prellberg T and Brak R 1993 *Phys. Rev. Lett.* **70** 951
- [13] Grassberger P and Hegger R 1995 *Journal de Physique I* **5** 597–606 URL <https://hal.archives-ouvertes.fr/jpa-00247085>